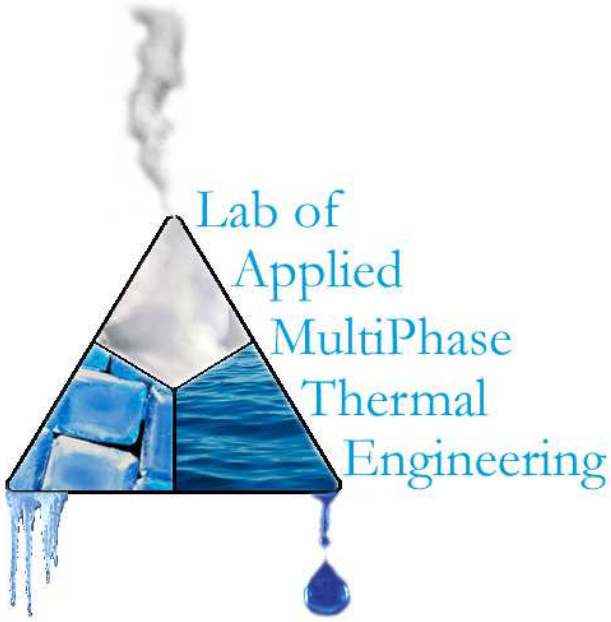

DALHOUSIE UNIVERSITY

Faculty of Engineering

Turbulent Scale and Wake Modeling on a Horizontal Axis Turbine: Final Report

Prepared as part of an awarded
OERA Open Call
(Nov 5th 2013 – Oct 3rd 2014)

By
Dr. Dominic Groulx, P.Eng, ing., Associate Professor
Nicholas Osbourne, MASc Candidate
Mechanical Engineering, Dalhousie University

December 12th 2014
Halifax, Nova Scotia, Canada

Executive Summary

One source of localized forces on tidal turbine blades, that can lead to lowered efficiencies and failures, is local turbulent eddies forming on and around the blades. These eddies, surviving in the wake, can also have a great influence on the performance and durability of other turbines downstream when in an array. At this time, very few experimental results of flow over turbines are available, with even less work done specifically on turbulence. In such circumstances, when few experimental tests are available, either because of cost or complications in such testing, numerical modeling is a great tool that enables initial studies and characterization for the flow, including strength of turbulence, size and distribution of flow structures, including eddies.

The work performed in this 1 year research project is the numerical modeling of the turbulent flow on a 3-blade horizontal axis turbine in order to study the size, strength and impact of turbulent eddies on the blades, the body of the turbine, and in the wake behind such turbine. In the wake, the turbulent perturbation in the flow behind a turbine will have a great impact on the efficiency, performance and durability of any turbine placed behind as is expected in an array.

This research project uses commercial CFD software (ANSYS CFX) to simulate flow over a 3-bladed turbine in order to test various numerical turbulence models and determine which one(s) are suitable for uses in tidal turbine flow analysis. Numerical results from the study also include flow field (velocities), pressure field and strength of turbulence. The numerical results will be validated with experimental results provided from the original group who made the experimental investigation of the tested turbine in Southampton. Such a validated study will provide a valuable tool to properly quantify turbulence shape and strength on any new tidal turbine design, leading to more robust, streamlined and safe design.

During the year-long period that this grant supported this project, the following research work has been done: a continuous literature review has been underway to ensure a full understanding of the flow physics involved and to gain further knowledge of similar research completed to date as well as best practices in this field of study. A fluid model was created using a turbine geometry that matched an experimental setup for model validation. Simulations were run for a range of tip speed ratios and compared using power and thrust coefficients. Methodology for building this model and result analysis are discussed later in this report. Overall results have good agreement in trends but both power and thrust are underestimated. Current geometry adjustment and mesh convergence studies are underway to investigate their impact on the model solution. Remaining work is discussed in the conclusion.

Table of content

List of figures

List of tables

List of Abbreviations and Variables

Greek Letters

ρ	Fluid Density [kg/m^3]
τ_w	Wall Shear Stress [Nm]
υ	Kinematic Viscosity [m^2/s]
ω	Rotational Velocity [rad/s]
Δy_P	First Node to Wall Distance

Variables

A	Turbine Swept Area [m^2]
A_P	Planform Area [m^2]
C_P	Power Coefficient
C_T	Thrust Coefficient
D	Turbine Diameter
F_L	Lift Force [N]
F_D	Drag Force [n]
k-ε	Turbulent Kinetic Energy – Turbulent Dissipation (Turbulence Model)
k-ω	Turbulent Kinetic Energy – Specific Dissipation (Turbulence Model)
P	Power [W]
Q	Torque [Nm]
R	Turbine Radius
Re	Reynolds Number
T	Thrust [N]
$V_{deficit}$	Velocity Deficit
V_0	Free-stream, Inflow Velocity [m/s]
V_W	Velocity in the wake [m/s]
y^+	Dimensionless Wall Distance (Y plus)

Abbreviations

CFD	Computational Fluid Dynamics
HATT	Horizontal Axis Tidal Turbine
LAMTE	Laboratory of Applied Multiphase Thermal Engineering
NACA	The National Advisory Committee for Aeronautics
SST	Shear Stress Transport (Turbulence Model)
TSR	Tip Speed Ratio

1 Introduction

The information contained hereof has been prepared by the Laboratory of Applied Multiphase Thermal Engineering (LAMTE) to report on work done between November 2013 and October 2014 as part of an OERA grant funded research. This research involves the investigation of wake characteristics and turbulent nature surrounding a horizontal axis tidal turbine (HATT).

1.1 Purpose

As seen in the Section 1.2, numerical modeling of turbulent flow is now studied and developed by more groups around the world; each still trying to understand the behaviour of the different turbulent models as they relate to the modeling of a tidal turbine. Very few of those models are applied to real-life experimental testing for validation, which is ultimately the aim of this work. This investigation addresses OERA's Marine Renewables Energy Research Targeted Research Priorities 4 and 5:

4. Monitoring and Optimizing Operational and Life-Cycle Performance of Turbines and Related Equipment: development of turbulence tidal flow and corresponding loads on subsea and marine equipment leading to development of optimal engineering design;

5. Monitoring Impacts Following Deployment of Turbines and Turbine Arrays: to understand how the performance of individual turbine or arrays are impacted by physical conditions (such arrays will not be installed in the short term, numerical simulations being the only reliable tool to study them at the moment).

1.2 Literature Review

Numerical simulation of tidal turbines is indisputably a powerful and essential tool for the development of the tidal power industry. With that being said there are many approaches and models available to the researcher, with new methods being continually introduced to reduce numerical deficiencies. The most common modeling approaches for tidal turbine simulation are the blade element theory [1], the momentum theory, the actuator disc theory [2] and computational fluid dynamics (CFD).

Blade element/momentum (BEM) [3, 4] (combination of blade element and momentum) methods, most commonly used in wind turbine performance analysis, have been shown to be insufficient for unsteady loading and, relevant to this research project, for producing a fine resolution of fluid flow in the wake of a tidal turbine [5]. The actuator disc theory is now generally coupled to BEM or CFD [6] to provide a more robust solution. This method still lacks the solution quality that would result from a standalone CFD model. A fully CFD approach has been shown to have the capability of resolving turbulence in the near and far field regions at fine resolutions for a three dimensional horizontal axis tidal turbine [7]. Direct Numerical Simulation (DNS) is possible but has an impractically high computational cost. To reduce simulation time the flow can be broken into steady and fluctuating components, requiring a turbulence model to resolve these perturbations. Currently research is being done to determine the most appropriate turbulence model to use in a tidal turbine CFD simulation.

The most commonly used turbulence models today are the *k-ε* and *k-ω* eddy-viscosity models, Shear Stress Transport (SST), the Launder-Reece-Rodi (LRR) Reynolds stress model and the Large Eddy Simulation (LES) model. The *k-ε* turbulence model is acceptable for initial use to reduce computational cost [8] but is insufficient by itself for detailed turbine simulation as it tends to underpredict force components [9]. The SST model utilizes *k-ω* in the inner boundary regions and *k-ε* in the free-stream regions. This model is capable of resolving turbulence within an acceptable margin of error [10], as is LRR [9]. A shortcoming of this level of turbulence modeling is an underprediction of the power coefficient. To achieve a higher resolution of the turbulence in the near and far regions, while requiring less computational effort than a Direct Numerical Simulation, an LES model can be used. LES has been proven as a viable option for tidal turbine turbulent simulations [11].

This research project aims to accurately simulate turbulent flow over a scaled horizontal axis tidal turbine to resolve turbulence in the near and far field regions. The simulation of a scaled model is an appropriate approach [1212] and allows for experimental validation [13]. Wake characteristic parameters, such as velocity deficit and turbulence intensity, are essential to future multi-turbine investigations as they will have direct impact on the efficiency and performance of subsequent downstream turbines. Vortex shedding is a dynamic phenomenon which would also impact performance, along with durability of such array turbines. Regional vortices and pressure differences can also be used to estimate loading on the blades and support structure. The successfully validated model will enable a better determination of which turbulence model is better suited for tidal turbine study, and will therefore be able to accurately estimate blade forces and near/far field turbulence. The success of this project will allow for improved blade design optimization as well as give better insight into the flow-physics of a tidal array setup.

2 Scientific Objectives

As defined in the original grant application, the three objectives of this work were:

1. Develop a numerical modeling methodology, using ANSYS CFX, enabling reliable study of turbulent flow over a horizontal axis turbine;
2. Validate the numerical models using experimental results from the University of Southampton and determine which turbulent model (*k-ε*, *k-ω*, SST) is the best suited for this application;
3. Characterize the nature of the turbulent flow around the turbine (size, shape and strength of eddies) and in the wake (length, zone of impact, strength of turbulence);

3 Methodology

3.1 2D Model Validation

A two dimensional model was created to validate the fluid physics applied in CFX. A four digit profile, NACA 1408, was chosen to compare to XFOIL, a theoretical airfoil design and analysis program created at MIT. A range of angles of attack were investigated (-7.5° to 15°). Lift and drag coefficients were used for this analysis and are defined as:

$$C_L = \frac{F_L}{\frac{1}{2}\rho A {V_0}^2} \quad (1)$$

$$C_D = \frac{F_D}{\frac{1}{2}\rho A {V_0}^2} \quad (2)$$

A chord length of 1 m was chosen, the fluid is water, and all simulations were defined such that Re = 500,000. Figure 1 provides a visual of the domain size, a case with 5° angle of attack.

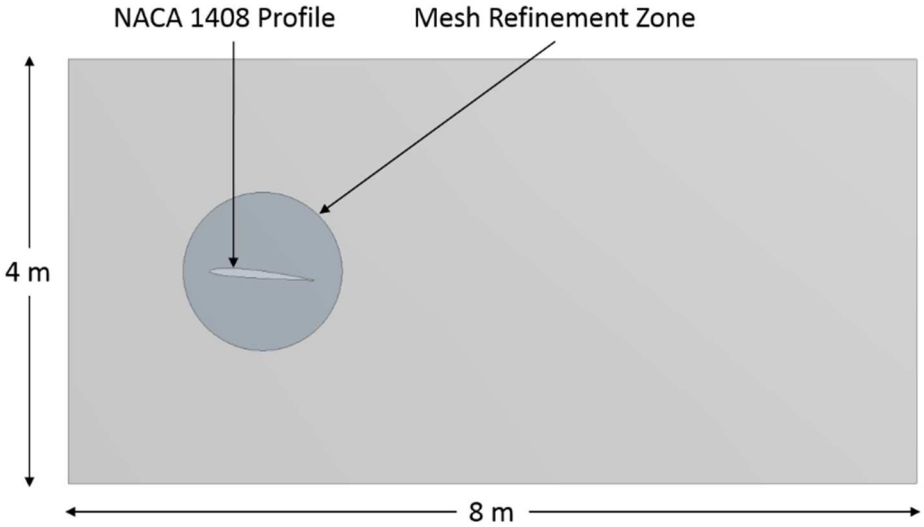

Figure 1: 2D Domain

All 2D models, results of which are presented in Section 4.1, incorporated a mesh of ≈ 370,000 cells and a $y^+ \approx 1$, a parameter defined and discussed in Section 3.3.2. A mesh refinement zone was incorporated to provide finer resolution in key areas of separation and eddy shedding. This methodology will be used in future three dimensional studies. Turbulence modelling and boundary conditions match that of the three dimensional models, save the symmetry walls, and are further discussed in Section 3.3.

3.2 Geometry

This investigation focussed on a three bladed horizontal axis tidal turbine; specifically, a geometry to match experiments from the University of Southampton. Blade parameters were provided by way of 17 cross-sectional profiles. Chord, pitch and thickness to chord ratios were given for varying radii and are provided au-dessous in Table 1.

Table 1. Blade Parameters [8].

r/R	*c/R*	Pitch Distribution [deg]	*t/c* [%]
0.20	0.1250	15.0	24.0
0.25	0.1203	12.1	22.5
0.30	0.1156	9.5	20.7
0.35	0.1109	7.6	19.5
0.40	0.1063	6.1	18.7
0.45	0.1016	4.9	18.1
0.50	0.0969	3.9	17.6
0.55	0.0922	3.1	17.1
0.60	0.0875	2.4	16.6
0.65	0.0828	1.9	16.1
0.70	0.0781	1.5	15.6
0.75	0.0734	1.2	15.1
0.80	0.0688	0.9	14.6
0.85	0.0641	0.6	14.1
0.90	0.0594	0.4	13.6
0.95	0.0547	0.2	13.1
1.00	0.0500	0.0	12.6

The experimental blades consisted of five, 6 series, NACA 63-8XX profiles: NACA 63-812, 63-815, 63-818, 63-821 and 63-824. A nominal scale profile was obtained and then twisted/scaled using Matlab to achieve the 17 sections shown in Figure 2.

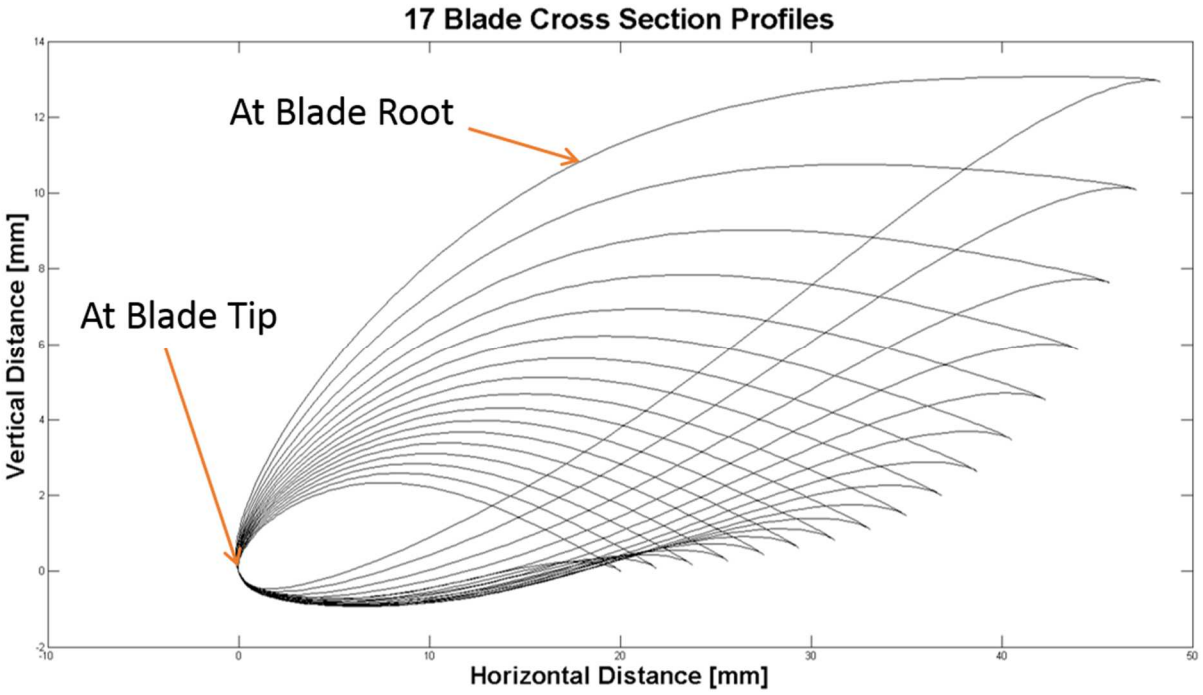

Figure 2: Blade Cross-Sectional Profiles

The fourth column in Table 1 presents the ratio of maximum thickness to chord, a ratio that is described in the last two digits of the 6 series NACA designation. The experimental blade has a relatively linear transition from root to tip so a linear transition was applied to the numerical blade. Figure 3 demonstrates the linear distribution method used in the Matlab code. The top value (*e.g.* r80) represents the radial distance from the hub centre in mm and the lower value (*e.g.* 21 x 1) represents the proportion of NACA 63-8XX used at that cross-section.

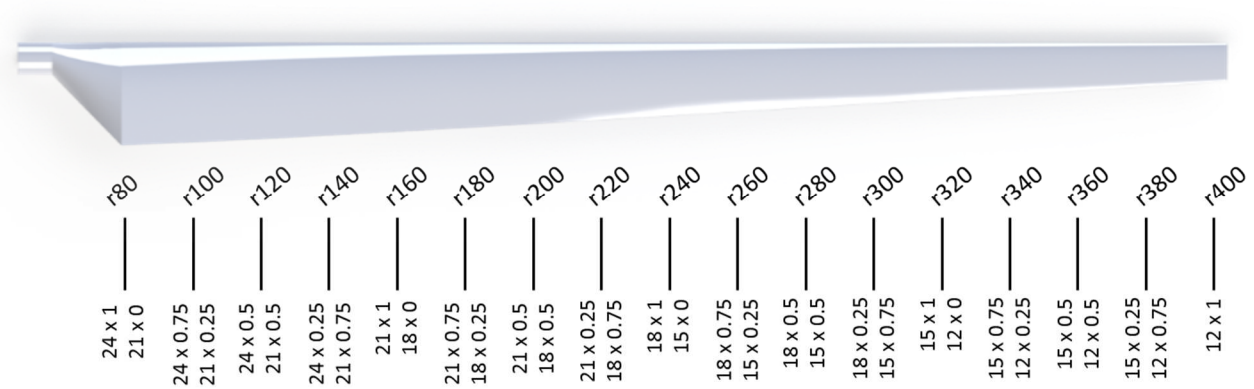

Figure 3: Linear Distribution Method

Figure 4 presents the three dimensional result that was built using SolidWorks. The blade geometry was designed as explained above while the nacelle and support structure dimensions were estimated from publications. A range of hub pitch angles (15°, 20°, 25°, 27° and 30°) had been measured using a digital inclinometer during experimentation, where here the angle is set numerically. This investigation focus on hub pitch angles of 20° and 25°.

Figure 4: 3D Blade and Turbine Geometries

3.3 Numerical Modelling

3.3.1 Fluid Domain

Experimental tests were completed, in 2007, in the cavitation tunnel at QinetiQ, Haslar and in the towing tank at the Southampton Institute. The cavitation tunnel test-set was chosen for validation purposes. Dimensions of the experimental setup are provided in Table 2. These are represented in the numerical fluid domain, save the tank length. Inlet and outlet lengths of 2*D* and 5*D* (where *D* denotes the turbine diameter) are used, respectively. This application is visually presented au-dessous in Figure 5.

Table 2. Cavitation Tunnel Parameters.

Parameter	Magnitude
Length	5 m
Breadth	2.4 m
Depth	1.2 m
Maximum Flow Speed	8 m/s

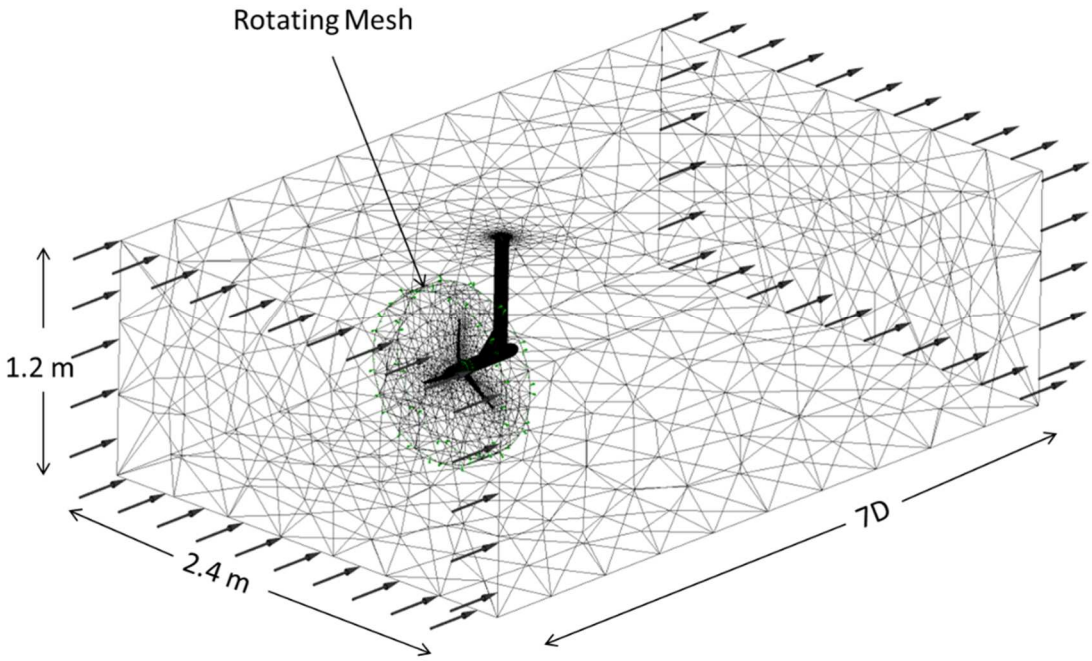

Figure 5: Computational Mesh

A disadvantage of experimental validation is the effect of blockage on fluid phenomena. Wake interaction with the tank walls will increase velocity through the turbine and give unrealistic results. Blockage corrections can be applied to give a free-stream estimate of the corresponding physics. A blockage correction factor can be applied as a numerical estimate, which is the case for the published experimental results. Another method, computationally, is to expand the domain cross-section area to approximate a free-stream flow. This method was applied and compared to the original results. The domain's height and width were both doubled in size. The results of this study are provided in Section 4.2.

3.3.2 Computational Mesh

The computational mesh was built in ANSYS Mesher using unstructured tetrahedral elements to allow for the best representation of the geometry. Figure 5 is a representative example of a mesh used. The majority of the domain is expressed as a stationary mesh, whereas a cylindrical mesh subdomain encapsulates the turbine and rotates at prescribed rates. The rotation rate is determined by achieving a desired tip speed ratio (TSR), a numeric that describes the relationship of the tangential blade tip velocity and the inflow velocity. It is calculated using the following relation:

$$\boldsymbol{TSR} = \frac{\boldsymbol{\omega R}}{\boldsymbol{V_0}} \tag{3}$$

Inflation layers are incorporated at the turbine and blade surfaces to better resolve the boundary layer flow, see Figure 6 for example. It was desired to numerically resolve the boundary layer rather than using wall functions. Wall functions apply empirical coefficients to the near wall flow to create a logarithmic estimate of the boundary layer. This approach benefits from requiring minimal mesh resolution at the wall but is insufficient for laminar to turbulent transition, as well as detailed investigations. Low Reynold's Method however fully resolves the boundary layer flow. This approach is more computationally intensive as it requires a high refinement of the mesh at the boundary. A convenient parameter that helps define the near wall method is the dimensionless wall distance y^+, colloquially called y plus, which is defined as:

$$\boldsymbol{y^+} = \frac{\boldsymbol{\Delta y_P}}{\boldsymbol{v}} \sqrt{\frac{\boldsymbol{\tau_w}}{\boldsymbol{\rho}}} \tag{4}$$

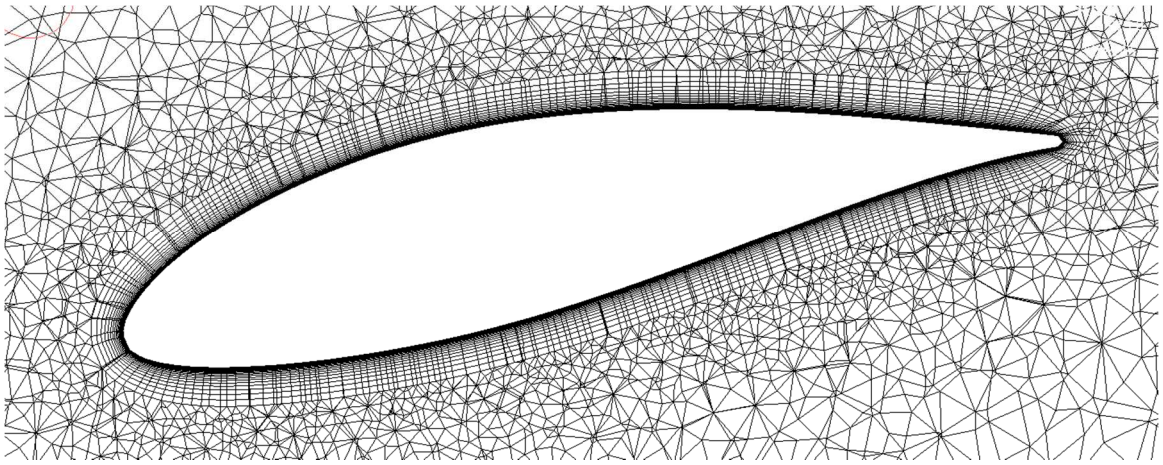

Figure 6: Computational Mesh – Inflation Layer on Blade

Full TSR range results presented in Section 4.2 incorporated a $y^+ < 100$ but subsequent studies have applied a $y^+ \approx 1$. Figure 7 provides a detailed view of the refined mesh at the hub and blade root. Standard boundary layer theory is used to estimate the wall shear stress and boundary layer thickness. The first node distance can then be derived by incorporating the desired number of inflation elements and the applied growth rate. The value for y^+ can then be post-processed in ANSYS CFD-Post, at which point meshing adjustments can be made if necessary.

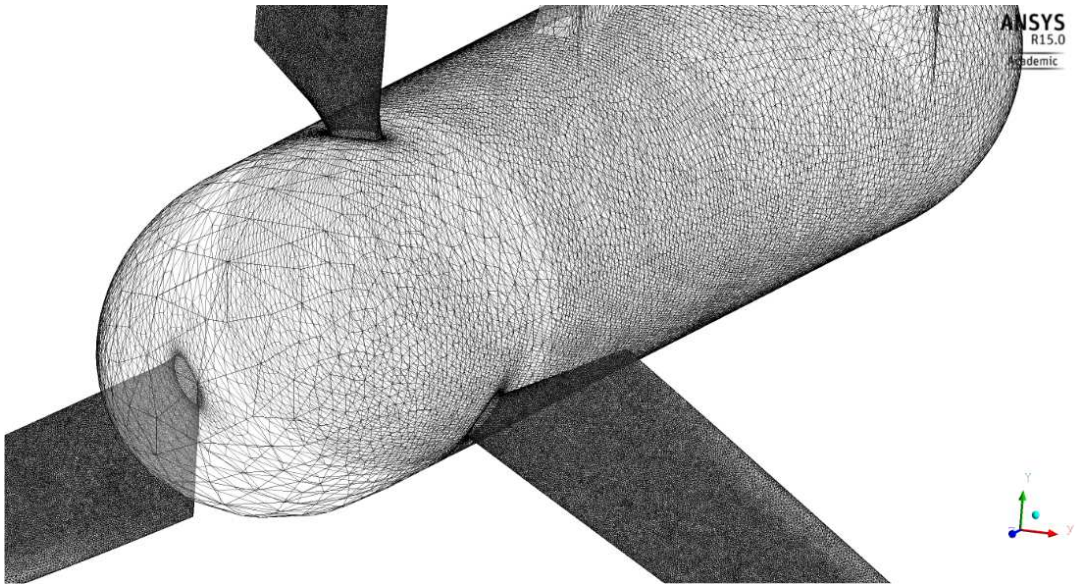

Figure 7: Computational Mesh – Turbine Close Up

A mesh convergence study is currently underway to ensure result independence of any finer spatial resolutions. Other geometry factors such as trailing edge bluntness and twist axis location are also being studied. Parameters such as y^+, maximum cell face size and mesh density directly behind the turbine are of interest. Currently these studies incorporate roughly 25,000,000 cells. Both the thrust and power coefficients are considered for convergence criteria. They are also used later for validation purposes. These are expressed in the following ways:

$$C_T = \frac{T}{\frac{1}{2}\rho A {V_0}^2} \tag{5}$$

$$C_P = \frac{P}{\frac{1}{2}\rho A {V_0}^3} = \frac{\omega Q}{\frac{1}{2}\rho A {V_0}^3} \tag{6}$$

In addition to global mesh resolution sensitivity, domain length and mesh density directly behind the turbine are also factors to be studied with a convergence study. For future transient analyses a time-step convergence study is also of import.

3.3.3 Turbulence Models

The Shear Stress Transport (SST) turbulence model was chosen for the bulk of this investigation, and the only one used so far, as it has been proven to have an acceptable balance between accuracy and computational effort (See Section 1.2). SST is a two equation eddy viscosity model comprised of the *k-ε* and *k-ω* models. An inherent transitional regime is used that applies *k-ω* in the inner boundary layer and *k-ε* when further in the free-stream. This approach negates the shortcomings of the individual models. A final comparative study, as part of the remaining work, will show the difference in results from these three models (*k-ε*, *k-ω*, SST).

3.3.4 Numerical Setup

The incorporated domain boundary conditions are provided in Table 3. The fluid domain incorporates a rotating cylindrical mesh, enveloping the turbine, seen in Figure 5. Steady state simulations were ran, the results of which will be used to initialize transient simulations.

Table 3. Boundary Conditions.

Boundary	Condition
Inlet	Normal Speed (1-1.7 m/s)
Outlet	P_{rel} = 0 Pa
Turbine Walls	No-Slip Condition
Domain Interfaces (Steady State)	Frozen Rotor
Domain Interfaces (Transient)	Transient Rotor Stator

4 Results

4.1 2D Results and Discussion

A two dimensional analysis of a NACA 1408 airfoil was run over a range of angles of attack. Both lift, Figure 8, and drag, Figure 9, coefficients showed good agreement until an angle of attack of 10°. This divergence from expected results is due to severe separation at high angles of attack, a fluid physics that is difficult to resolve numerically. Low angle of attack agreement is sufficient as the three dimensional focus avoids high angles of attack. Figure 8b and Figure 9b compare the results from a range of angles of attack of -7.5° to 7.5°. This region had an average relative difference of 13% and absolute difference of 0.001 for lift coefficient and 39% and 0.007 for drag coefficient. This result is acceptable as lift coefficient directly relates to power output in three dimensional studies.

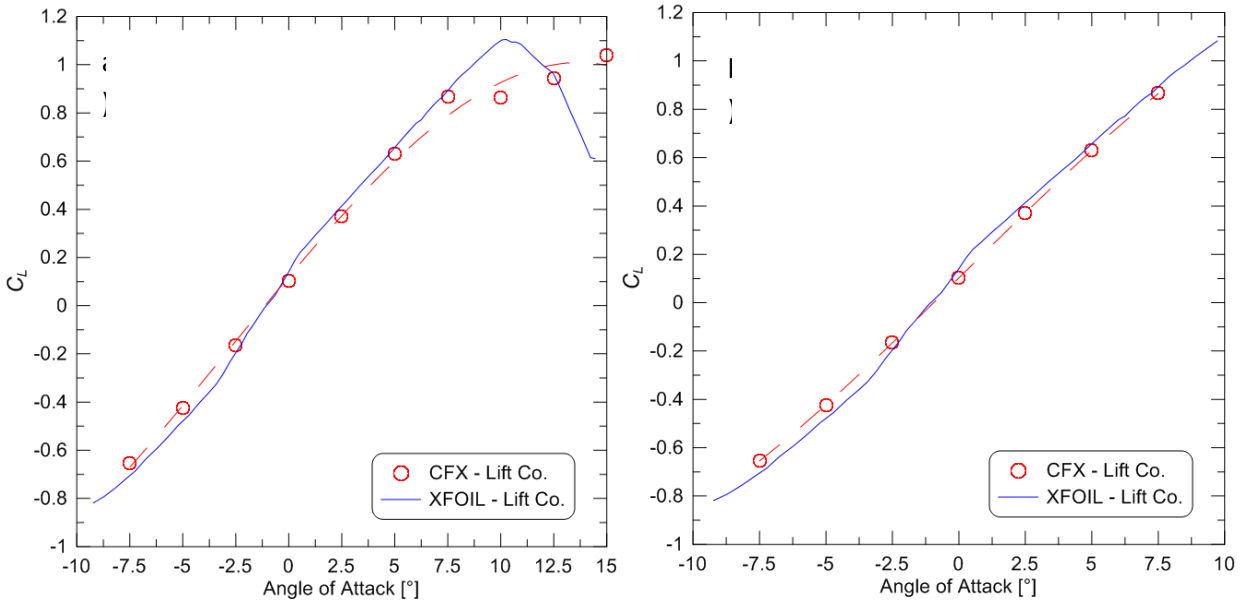

Figure 8: Lift Coefficients – (a) Full Range (b) Stable Range

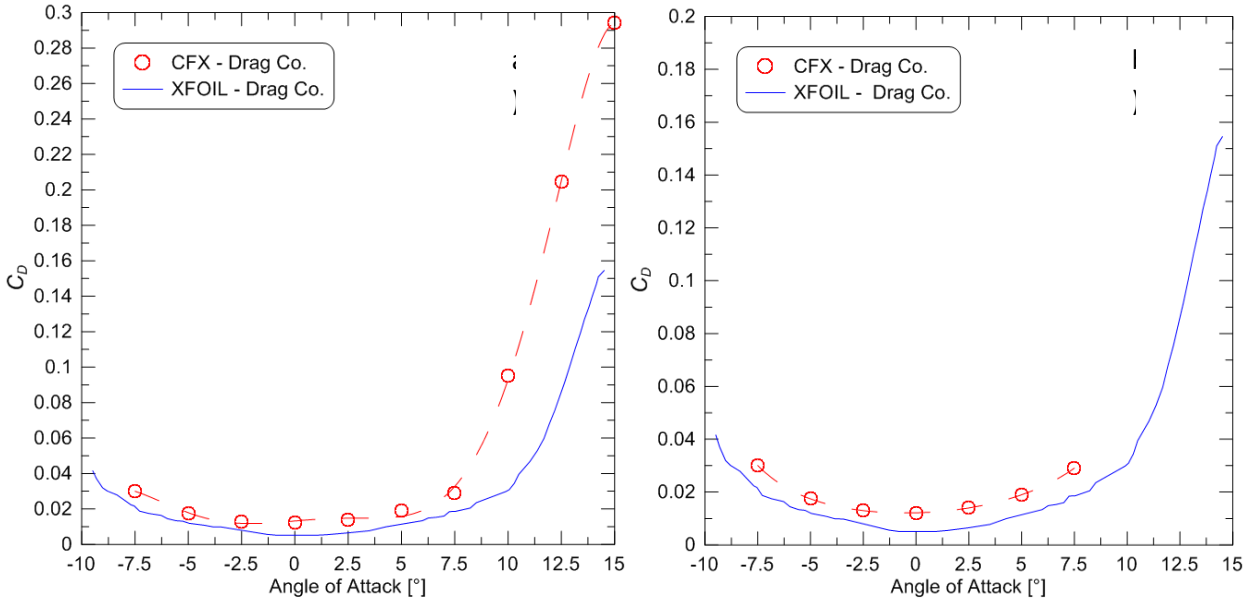

Figure 9: Drag Coefficients – (a) Full Range (b) Stable Range

4.2 3D Results and Discussion

4.2.1 Validation

All data for comparison are taken from research done at the University of Southampton [14] . Figure 10a and Figure 10b show C_P and C_T as a function of TSR, respectively, for the 25° hub pitch configuration. Experimental comparisons show good agreement in prediction trends but both are under-estimated. The predicted C_P curve has a peak of 0.25 at TSR = 5 with average relative and absolute differences of 48% and 0.14, respectively, below experimental values. The thrust coefficient has a peak of 0.35 at TSR = 5.5 with average relative and absolute differences of 36% and 0.18.

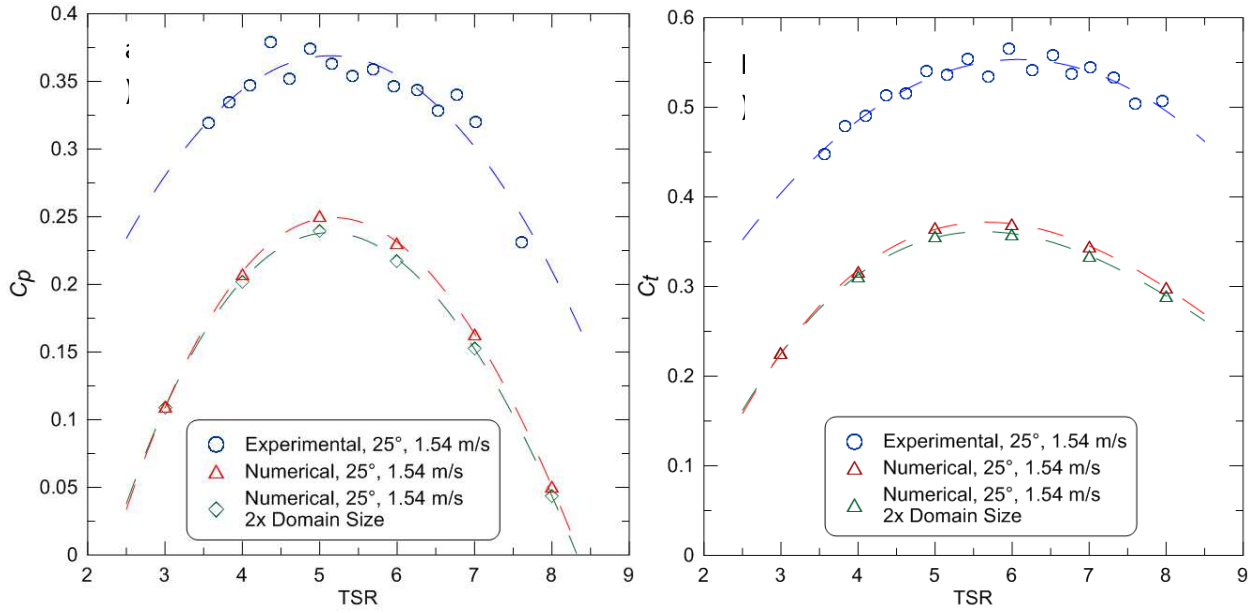

Figure 10: Power (a) and Thrust (b) Coefficients

This under-prediction could be attributed to several factors, of which include the impact of the mesh density, near and far wake mesh resolution, insufficient downstream domain length and blockage introduced by the smaller numerical domain. Two other geometrical factors which are currently being studied are twist axis location and trailing edge bluntness. Preliminary results of twist axis location shown an improvement in power coefficient agreement. Figure 11 shows power coefficient output for a variety of twist axis location scenarios. Current results show that the solution is greatly affected when the twist axis is moved away from the leading edge but tends to be relatively independent thereafter.

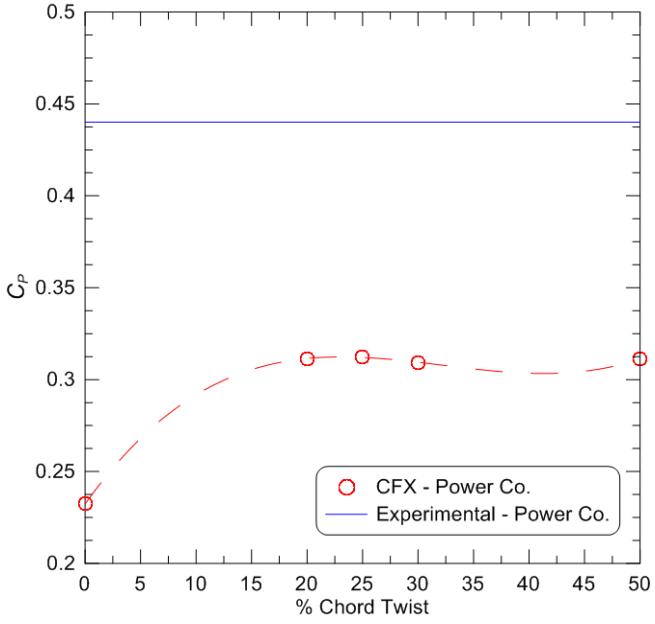

Figure 11: Twist Axis Analysis, 20°, 1.73 m/s

As stated in Section 3.3.1 the experimental results were corrected for blockage. To begin a free-stream approximation in the numerical simulations, the tank width and height were doubled. The results of C_P and C_T results of this were also presented in Figure 10. As expected, both the thrust and power coefficients dropped due to the reduced impact of blockage. The doubling of domain size reduced C_P and C_T by 6% and 2% from the original numerical result.

It is interesting to note that peak power and torque do not occur simultaneously, observable in Figure 12. This is due to the non-linear relationship, shown au-dessous. A peak power of 230 W at TSR = 5 and peak torque of 12.5 Nm at TSR = 4.5 were observed.

$$\boldsymbol{P = \omega Q} \tag{7}$$

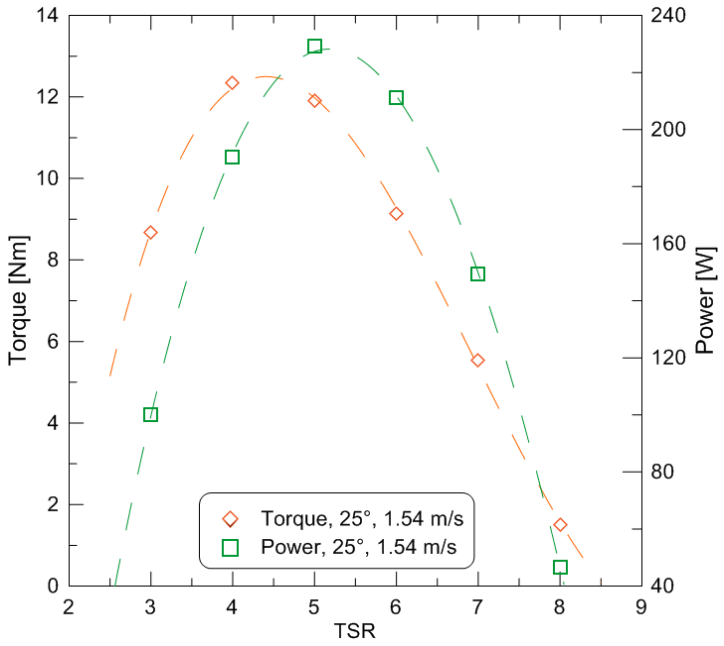

Figure 12: Power and Thrust

4.2.2 3D Results

Figure 13 shows a pressure contour plot, highlighting key areas of high and low pressures. Note the pressure differential between the upstream and downstream zones at the turbine blade. It is this differential that gives lift, torque, and ultimately power. There is also a notable effect caused by the nacelle, with zones of high pressure above and low pressure below. Local velocity values are also presented in Figure 13, where the length and color signify the magnitude. An increase in fluid velocity is seen at the turbine blade, related to the pressure differential. In addition, a stagnation point can be seen directly behind the support structure. It is at this area that large amounts of eddy shedding would take place.

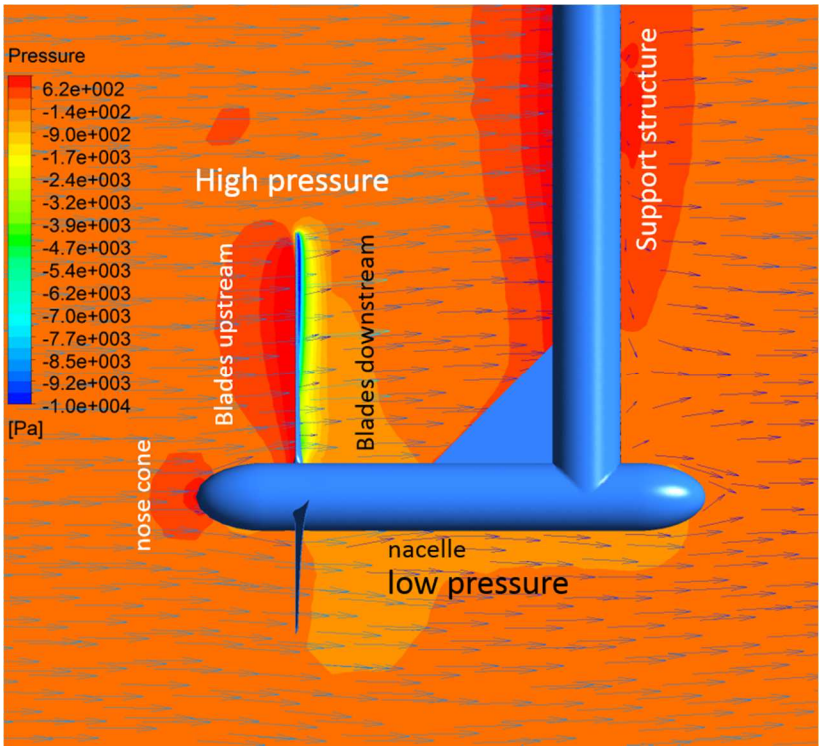

Figure 13: Pressure Contour, 25°, 1.54 m/s

Velocity deficit, a non-dimensional number relating downstream and free-stream velocities, is defined with the relationship au-dessous. This parameter is an important post-processing tool for quantifying downstream wake recovery distances. Figure 14 shows that with the current numerical setup most wake turbulence has dissipated by five diameter lengths downstream, at which point the velocity profile matches the inflow velocity. Fluctuations in the one diameter length deficit are due to fluid interactions with the nacelle.

$$V_{deficit} = 1 - \frac{V_W}{V_0} \tag{8}$$

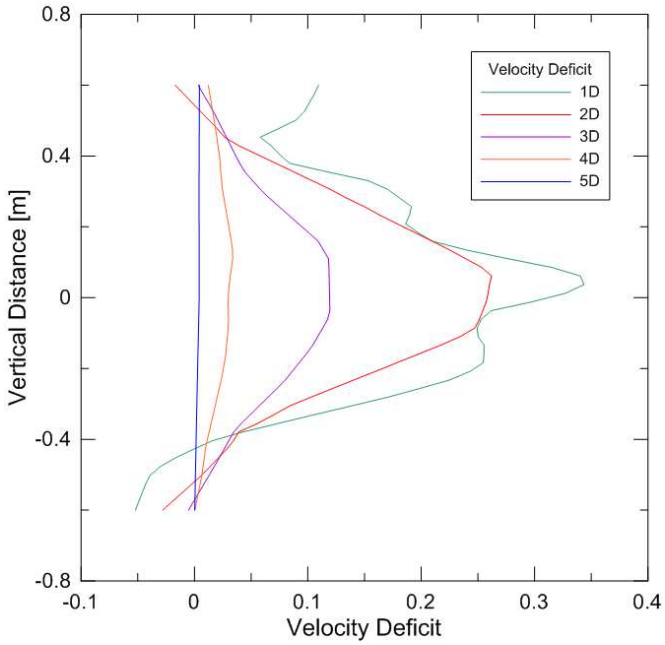

Figure 14: Velocity Deficit, 25°, 1.54 m/s

Figure 15 presents the absolute helicity in orange. Vortex creation is seen focused at the blade root and tip, two areas of abrupt blade geometry changes. These two areas are primary components of wake turbulence and are associated with turbine drag.

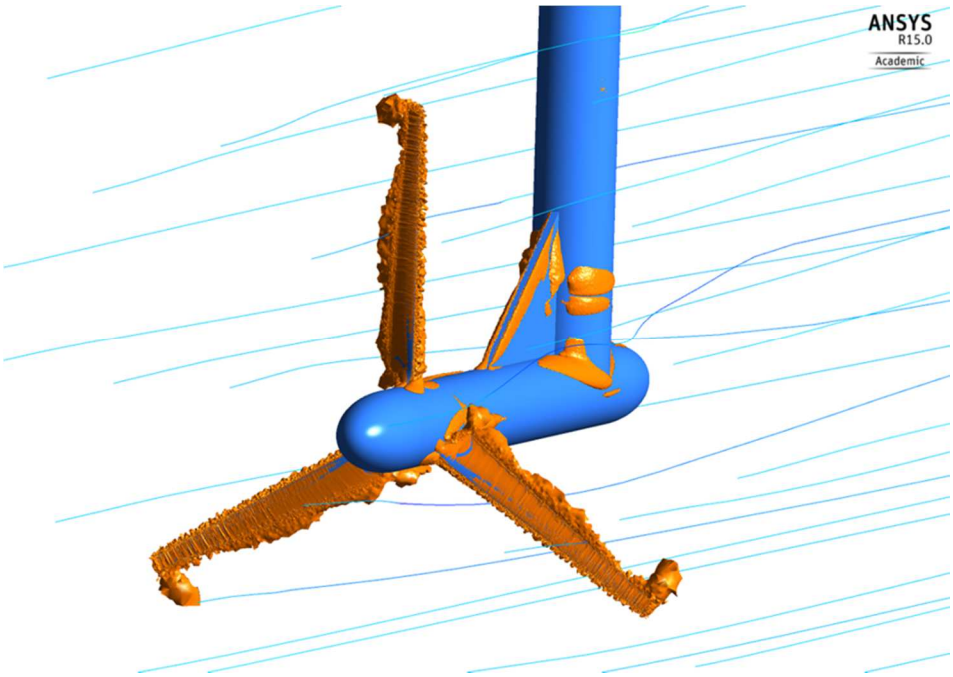

Figure 15: Absolute Helicity, 25°, 1.54 m/s

accepted for publication. Finally, as mentioned in the interim report, the connection to NRC St-John's was initially misleading so a trip there will not be required.

8 Employment Summary

Two researchers have been involved on this project as shown on table 5.

Table 5 Employment Summary

Name	Position	Student	Scientific Contribution	Duration on Project
Nicholas Osbourne (Full time)	MASc Student	Yes (MASc)	- Performs numerical modeling and research - Result analysis and presentation - Abstract and paper writing	Sept. 2012 (one year prior to OERA grant)
Dr. Dominic Groulx (Full time – no salary from grant)	Associate Professor	No	- Principal investigator and research surpervisor - Abstract and paper writing	

9 Conclusions and Recommendations

A two dimensional numerical model of flow over an airfoil has successfully been created. This was done as a simplified case to ensure the right amount of forces (lift and drag) where generated and calculated through CFX. Lift coefficient had excellent agreement between -7.5° and 7.5° angles of attack with relative and absolute differences of 13% and 0.001, respectively. Likewise, drag coefficient between these angles has relative and absolute differences of 39% and 0.007. A severe separation develops beyond these angles and numerics become unsteady. This is acceptable as the three dimensional case avoids this flow scenario.

The simple 2D validation then led to the three dimensional model of a three bladed horizontal axis tidal turbine. In comparison to experimental results, the numerical solution has reasonable agreement in trends when considering both thrust and power coefficients. A significant under-prediction is observed for both of these parameters however, with a relative difference of 48% for the power coefficient and 36% for thrust coefficient. Current work involves analyzing the impact of twist axis location. Figure 11 shows the preliminary impact on the power coefficient result. Adjusting the twist axis from 0% to 25% along the chord reduced the relative difference from 48% to 29%.

Looking at the three objectives defined in section 2, the following has been done so far:

1. Both 2D and 3D numerical modeling methodologies, using ANSYS CFX, were put forward and used to calculate forces acting on the geometries as well as enabling turbulent flow studies;
2. The numerical model is in the process of being validated using experimental results from the University of Southampton. Work is still on-going to improve the level of agreement between numerical and experimental results. Only one turbulence model (SST) has been used up to this point;
3. The turbulent flow around the turbine has been partly characterized (size, shape and strength of eddies). The same can be said of the wake (length, zone of impact, strength of turbulence). On-going work is refining the accuracy of the results in both region and will lead to a more accurate characterization;

9.1 Remaining Work

The following work is still required to bring to project to completion:

- ✓ Completion of mesh convergence study. This is currently underway, investigating the effects of adjusting y^+, maximum cell face size and mesh density directly behind the turbine. To have confidence in CFD results, it must be shown that the fluid numeric are independent of finer spatial resolutions.
- ✓ A full set of simulations will then be rerun for comparison with experimental values from the University of Southampton.
- ✓ A complete post-processing analysis will then be done in ANSYS CFD-Post. This will incorporate velocity deficit, velocity and pressure gradients contours, turbulence intensity contours, wake recovery distance contours, and 3D helicity.
- ✓ Employ k-ε and k-ω turbulence models for comparison to Shear Stress Transport results.

References

1. Wilson, R.E. and P.B.S. Lissaman, *Applied Aerodynamics of Wind Power Machines*, 1974, Oregon State University. Supported by the National Science Foundation, Research Applied to National Needs. p. 117.
2. Harrison, M.E., et al. *A comparison between CFD simulations and experiments for predicting the far wake of horizontal axis tidal turbines*. in *The 8th European Wave and Tidal Energy Conference*. 2009. Uppsala, Sweden.
3. Batten, W.M.J., et al., *The prediction of the hydrodynamic performance of marine current turbines.* Renewable Energy, 2008. **33**(5): p. 1085-1096.
4. Bahaj, A.S., W.M.J. Batten, and G. McCann, *Experimental verifications of numerical predictions for the hyrodynamic performance of horizontal axis marine current turbines.* Renewable Energy, 2007. **32**: p. 2479-2490.
5. Lee, J.H., et al., *Computational methods for performance analysis of horizontal axis tidal stream turbines.* Applied Energy, 2012. **98**: p. 512-523.
6. Bai, G., et al., *Numerical investigations of the effects of different arrays on power extractions of horizontal axis tidal current turbines.* Renewable Energy, 2013. **53**: p. 180-186.
7. O'Doherty, T., et al. *Experimental and Computational Analysis of a Model Horizontal Axis Tidal Turbine*. in *The 8th European Wave and Tidal Energy Conference*. 2009. Uppsala, Sweden.
8. Masters, I., et al., *The influence of flow acceleration on tidal stream turbine wake dynamics: A numerical study using a coupled BEM–CFD model.* Applied Mathematical Modelling, 2013. **37**(16-17): p. 7905-7918.
9. McNaughton, J., et al., *CFD Predicition of Turbulent Flow on an Experimental Tidal Stream Turbine using RANS modelling*, in *The 1st Asian Wave and Tidal Energy Conference Series*2012: Jeju Island, Korea. p. 8 p.
10. McSherry, R., et al., *3D CFD modelling of tidal turbine performance with validation against laboratory experiments*, in *The 9th European Wave and Tidal Energy Conference*2011: Southampton, UK. p. 7 p.
11. Afgan, I., et al., *Turbulent flow and loading on a tidal stream turbine by LES and RANS.* International Journal of Heat and Fluid Flow, 2013. **43**: p. 96-108.
12. Mason-Jones, A., et al., *Non-dimensional scaling of tidal stream turbines.* Energy, 2012. **44**(1): p. 820-829.
13. Kang, S., et al., *Numerical simulation of 3D flow past a real-life marine hydrokinetic turbine.* Advances in Water Resources, 2012. **39**: p. 33-43.
14. Bahaj, A.S., et al., *Power and thrust measurements of marine current turbines under various hydrodynamic flow conditions in a cavitation tunnel and a towing tank.* Renewable Energy, 2007. **32**(3): p. 407-426.

Appendix A

Nova Scotia R&D Energy Forum - Abstract

THREE DIMENSIONAL SIMULATION OF HORIZONTAL AXIS TIDAL TURBINE

Nick Osbourne
Research Advisor: Dominic Groulx

Department of Mechanical Engineering, Dalhousie University

This abstract is for submission to the Nova Scotia Energy R&D Conference 2014 – Energy for Change in the category of Marine Renewable Energy.

Demand for renewable energy continues to rise worldwide. Compared to some popular renewable energy sources, tidal energy has high power density and predictability. In-stream tidal energy is an emergent technology with great opportunity globally. Technological and environmental issues are numerous, however, and require innovation and inspiration to be overcome. These issues are a challenge for design testing but further fundamental knowledge is necessary to help tidal energy become a burgeoning industry.

Small scale experiments and numerical modelling of designs are far cheaper and quicker methods of evaluation. Designers are able to test their prototypes by utilizing these two approaches simultaneously. Experimental results can be used to validate numerical models. Key parameters can then be adjusted for turbine optimization or investigation of enigmatic phenomena.

This study aims to accurately produce three dimensional numerical simulations, in ANSYS CFX, of a three bladed horizontal axis turbine (HATT). The resultant power and thrust coefficients of these simulations will be compared to experimental results [1] at various tip speed ratios (TSR = 2-12) and blade root angles (15°-30°). Near and far field wake propagation will also be investigated. In addition to these variances, three common turbulence models will be applied for insight into their HATT application suitability. The results of this study will provide: validation of experimental results, further information on the turbulent flow in the near and far wake fields, and possible implications on the effectiveness of tidal arrays.

The turbine geometry in question has a design that matches experimental studies. The 800 mm diameter turbine, varying in pitch angle, has a blade geometry that interpolates five NACA profiles. The rotational velocity of the turbine is determined by the desired TSR (2-12). The total transient simulation time, up to 10 seconds, is chosen by allowing the turbine to complete ten full revolutions.

This investigation is ongoing and a mesh convergence study is currently underway. The resultant power and thrust coefficients are within a reasonable magnitude of experimental. An example of the streamline result is presented below. The completion of these simulations will provide further insight into the usefulness of numerical modelling in the tidal energy industry.

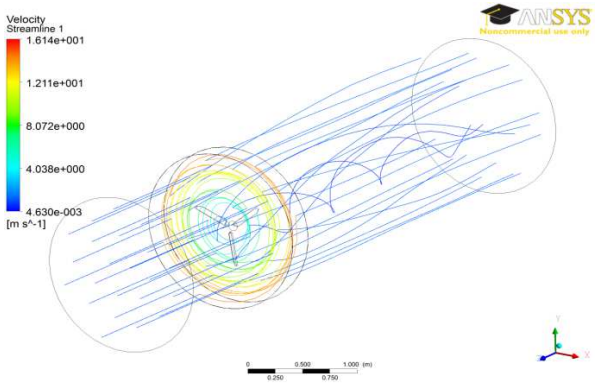

[1] A.S. Bahaj et al., “Power and thrust measurements of marine current turbines under various hydrodynamic flow conditions in a cavitation tunnel and a towing tank”, *Renewable Energy*. 32, 2007, pp. 407-426.

Appendix B

2nd AWTEC – Paper

THREE DIMENSIONAL SIMULATION OF A HORIZONTAL AXIS TIDAL TURBINE – COMPARISON WITH EXPERIMENTAL RESULTS

Nick Osbourne[1], Dominic Groulx[1], Irene Penesis[2]
[1]Department of Mechanical Engineering, Dalhousie University, Halifax, B3H 4R2, Canada
[2]Australian Maritime College, and institute of the University of Tasmania, Launceston, 7250 Australia

This paper presents the result of three dimensional numerical simulations of a three bladed horizontal axis tidal turbine (HATT). The Reynolds Averaged Navier Stokes (RANS) Shear Stress Transport (SST) turbulence model is studied and compared for the HATT simulation application. The resultant power and thrust coefficients of these simulations are compared to experimental results at various tip speed ratios (TSR = 3-8) with a blade root angle of 25°. Near field and far field wake propagation is investigated: for TSR 5 and 8, the turbine wake, as seen from the vorticity and resulting velocity plots, only survives for a length equivalent to two turbine diameter.

Keywords: Computational Fluid Dynamics (CFD), Horizontal Axis Tidal Turbine (HATT), Turbulence Models, Reynolds Averaged Navier-Stokes (RANS), Tip Speed Ratio (TSR)

INTRODUCTION

Global concerns of climate change, along with the cost of conventional fossil fuels, are rising. A result of this is the increasing emphasis on the advancement of renewable energy industries. Some of these industries, such as on-shore wind, are relatively well established. For example, optimal turbine, generator and tower designs, along with installation and upkeep methodologies, are well accepted. Marine energy industries on the other hand are untapped energy sources and perceptions of optimal designs vary. Fortunately initial stage complications can be reduced with lessons learned from other industries.

Marine energy industries come with their own challenges. For instance, in-stream tidal power difficulties include: salinity, extreme turbulence and fluid density, environmental issues and poor accessibility. Accessibility issues include installation along with scheduled and unscheduled maintenance calls. It is believed that the payoff is worth the effort however. It has been shown using two-dimensional, finite element, numerical simulations that 7 GW of power can be extracted from the Bay of Fundy–Gulf of Maine system using in-stream tidal turbines. Although extracting this total power produces significant tidal effects, it is estimated that 2.5 GW can be extracted with a maximum tidal amplitude change of 5% at any location in this system [1].

In marine energy industries, particularly in-stream tidal, reliability is the key. Turbine developers are more and more focusing on pre-deployment testing. Scaled testing allows for design parameter variation studies. At the Memorial University of Newfoundland, Alam and Iqbal conducted a series of flume tank experiments to analyze the effectiveness of a hybrid Darrieus and Savonius turbine designs [2]. Results were positive showing much desired low cut-in flow speeds. Similarly, Kirke *et al.* studied design variations of a straight blade Darrieus style hydrokinetic turbine [3]. Their findings from their real-world experiments showed an increased power by a factor of 3 in some configurations.

This testing can be combined with numerical investigations. The experimental results can be used to, not exclusively, validate the numerical model. The model can then be extrapolated to suit the geometry parameters and fluid regimes of the design scenario. Two prominent numerical approaches are the blade element momentum theory (BEMT) and computational fluid dynamics (CFD).

BEMT, originally utilized in wind turbine analyses, divides the turbine blade into a number of elemental 2D sections. This approach determines drag and lift forces for each section and integrates these across the blade to achieve thrust and power coefficients. Batten *et al.* completed a validation study of a HATT using BEMT with good agreement to experimental results [4]. This method however is based strictly on steady flow and does not account for wake expansion.

CFD approaches are more robust in that they can provide greater detail of the wake region as well as flow phenomena close to the turbine. McSherry *et al.* successfully created a RANS based CFD HATT model to compare against experimental results [5]. The model is later planned to be scaled up to determine hydrodynamic loads on a tidal turbine, the results of which will affect the design of the system drive train.

This process can also be reversed in that the models can predict optimal designs prior to testing. O'Doherty *et al.* studied seven variations of a horizontal axis tidal turbine using a CFD approach. The optimal design was then chosen for flume tank experiments; the results of which compare well to their numerical results [6].

A three dimensional fluid numerical model of a three bladed horizontal axis tidal turbine is currently under development. ANSYS-CFX, which incorporates RANS modelling, was chosen as a software platform as it is commercially available and had been proven to be applicable to similar scenarios [5, 7]. Model validation will be completed through comparison with a set of experiments performed at the University of Southampton [8]. Two areas of interest will be studied in the long term after a successful validation: a wake propagation scale and intensity study will provide insight on the appropriateness of turbine arrays and a characterization of local turbulent eddies will provide an estimate for structural load patterns on the blades. However, this paper will be limited to presenting the early findings of this study with a particular focus on vorticities and velocities in the wake of the turbine at tip speed ratios (TSR) of 5 and 8.

TURBINE GEOMETRY

This investigation focusses on a three bladed horizontal axis tidal turbine. Blade geometry parameters were provided in the publication from the University of Southampton [8]. These were given by way of 17 cross-sectional chord and pitch values at varying radii and have been provided in Table 1.

The experimental blade geometry was comprised of five NACA profiles (63-812, 63-815, 63-818, 63-821 and 63-824). The transitional period between these profiles was ambiguous however, so a consistent profile of NACA 63-815 was chosen for this investigation. A nominal profile was attained and implemented in a Matlab code, in which it was scaled and twisted to represent the 17 sections. Figure 1 presents the resulting profiles.

Table 1. Blade Parameters [8].

r/R	c/R	Pitch Distribution [deg]
0.20	0.1250	15.0
0.25	0.1203	12.1
0.30	0.1156	9.5
0.35	0.1109	7.6
0.40	0.1063	6.1
0.45	0.1016	4.9
0.50	0.0969	3.9
0.55	0.0922	3.1
0.60	0.0875	2.4
0.65	0.0828	1.9
0.70	0.0781	1.5
0.75	0.0734	1.2
0.80	0.0688	0.9
0.85	0.0641	0.6
0.90	0.0594	0.4
0.95	0.0547	0.2
1.00	0.0500	0.0

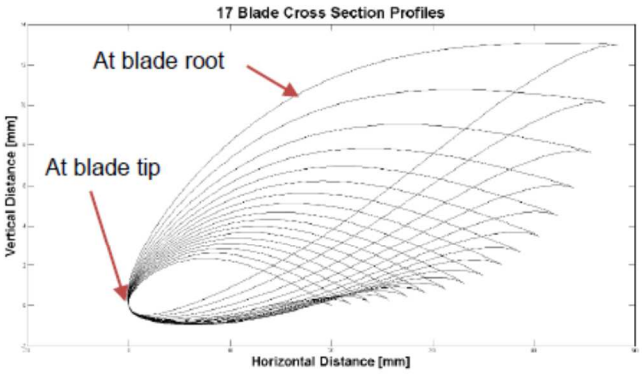

Fig. 1. Blade Cross-Sectional Profiles.

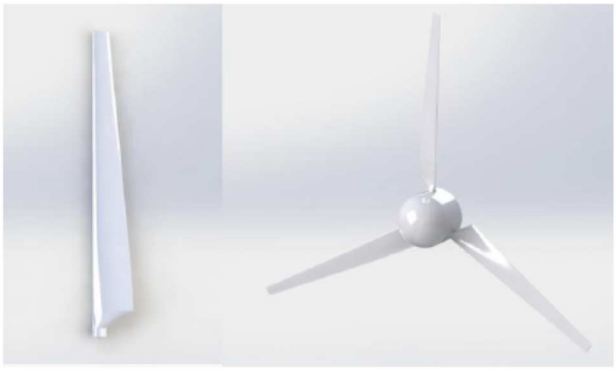

Fig. 2. Blade and Turbine Rendering.

These profiles were exported and lofted in SolidWorks to create the three dimensional geometries shown in Fig. 2. The hub diameter is 100 mm but currently the turbine nacelle is in consideration for final simulations. A range of hub pitch angles (15°, 20°, 25°, 27° and 30°) were measured experimentally using a digital inclinometer. This study uses only one hub pinch angle: 25°. It was achieved virtually by adjusting the angle between the plane of rotation and the chord of the first cross-sectional plane.

NUMERICAL MODELING

Fluid Domain

Experimental tests were completed in the cavitation tunnel at QinetiQ, Haslar and in the Towing Tank at the Southampton Institute [8]. For the purposes of this study only the towing tank experiments will be investigated. The dimensions of this tank are provided in Table 2. These are represented in the numerical fluid domain, except for the tank length. Currently inlet and outlet domain lengths are set to $2D$ and $5D$, respectively, where D denotes the rotor diameter. An outlet domain length study will later verify numerical independence of this parameter. A second series of simulations in an "open water" geometry will be performed to assess the amount of flow blockage simulated in the tow tank size system.

Table 2. Towing Tank Parameters [8].

Parameter	Magnitude
Length	60 m
Breadth	3.7 m
Depth	1.8 m
Maximum carriage speed	4.5 m/s

Turbulence Models

The Shear Stress Transport (SST) turbulence model will be used for the majority of this investigation. This is a two equation eddy viscosity model that comprises of the k-ε and k-ω models. SST employs k-ω in the inner boundary layer and transitions to k-ε further into the free stream. This approach negates the shortcomings of each model. A small comparison study will be done at the completion of this investigation to demonstrate the difference in turbulence model results in an in-stream tidal simulation application.

Computational Mesh

ANSYS Mesher was used to discretize the fluid domain for this study. The mesh consists of unstructured tetrahedrals to allow for improved representation of the geometry. A finely resolved cylindrical mesh encompasses the turbine and rotates at varying speeds to achieve desired TSR's. This cylinder lies within a larger stationary box which resembles the experimental setup. An example of the computational mesh is given in Fig 3. The rotating mesh was simulated using a General Grid Interface (GGI) inherent to ANSYS. This places an interface between the rotating and stationary domains over which flow properties are calculated.

Inflation layers were incorporated at the turbine blade surfaces to better resolve the boundary layer flow. An appropriate first layer thickness was applied to achieve a $y+ < 100$, an acceptable level for this investigation [7]. Figure 4 provides a detailed view of the hub and blade root.

Figure 5 presents a blade cross section view, demonstrating the high level of refinement at the blade surface while Fig. 6 provides a detailed view of the mesh at the leading edge. This example incorporates five inflation layers with a growth rate of 1.4.

A mesh convergence study is currently underway to ensure result independence of any finer spatial resolutions. Key meshing parameters that are of focus are: maximum mesh face size, minimum mesh face size, cell growth rate, curvature normal size, maximum inflation layer thickness, number of inflation layer cells and inflation layer growth rate. The results of this study will be disseminated in future publications.

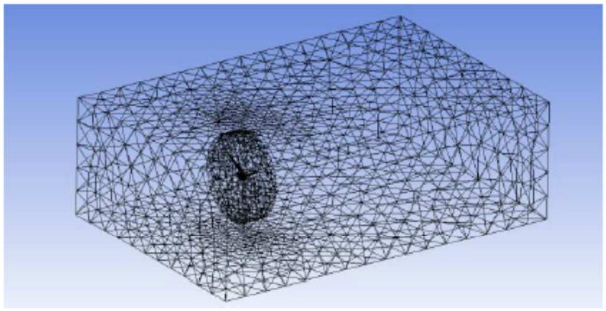

Fig. 3. Computational Mesh.

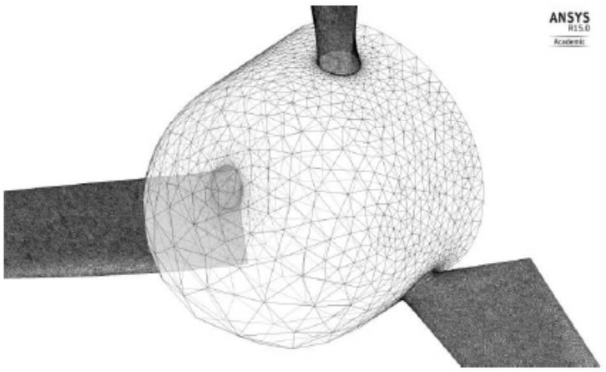

Fig. 4. Detailed View of Hub and Blade Roots.

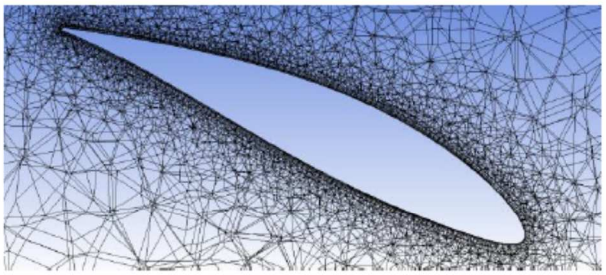

Fig. 5. Detailed View of Blade Cross Section.

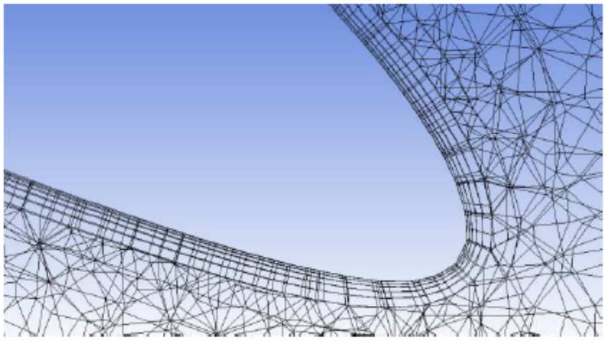

Fig. 6. Detailed View of Leading Edge.

A time-step convergence study will follow this study for subsequent transient simulations. Similar to mesh convergence, a time-step convergence study will determine the point of temporal independence of finer time-step resolutions. However, time-steps vary between runs as rotation rates differ between TSR scenarios. The approach will be to set time-steps that correspond to an angular rotation and reduce this value.

Both the thrust and power coefficients will be considered for convergence criteria. They are also in the next section for comparison with experimental results. These are expressed in the following ways:

$$C_T = \frac{T}{\frac{1}{2}\rho A U^2} \quad (1)$$

$$C_P = \frac{P}{\frac{1}{2}\rho A U^3} = \frac{\omega Q}{\frac{1}{2}\rho A U^3} \quad (2)$$

Where T and P are the thrust and power produced, respectively, ρ and U are the fluid density and upstream velocity, A is the rotor swept area, ω is the rotational speed in rad/s, and Q is the rotor torque.

Numerical Setup

The incorporated domain boundary conditions are provided in Table 3. The fluid domain incorporates a rotating cylindrical mesh, enveloping the turbine, seen in Fig. 3. Steady state simulations results are used to initialize transient simulations.

The rotational speed of the cylindrical domain is set to achieve a desired TSR, as defined below:

$$TSR = \frac{\omega R}{U} \quad (3)$$

Where ω is the rotational speed in rad/s, R is the turbine radius (400 mm), and U is the average upstream velocity.

EXPERIMENTAL COMPARISON

Preliminary experimental comparisons show good agreement in prediction trends. All experimental data for comparison are taken from research by Bahaj *et al.* [8].

Table 3. Boundary Conditions.

Boundary	Condition
Inlet	Normal Speed (0.8 – 2 m/s)
Outlet	P_{rel} = 0 Pa
Outer Walls	Free-Slip Condition
Turbine Walls	No-Slip Condition
Domain Interfaces (Steady State)	Frozen Rotor
Domain Interfaces (Transient)	Transient Rotor Stator

It should be noted that the results from these tests were corrected for blockage while the numerical results were not. Figure 7a shows C_p as a function of TSR and Fig. 7b, C_t versus TSR. Both C_p and C_t follow a similar trend as the experimental results but both are under-estimated. The predicted C_p curve has an average relative difference of 39% and average absolute difference of 0.12 below experimental values. Likewise, the predicted C_t curve has an average relative difference of 29% and average absolute difference of 0.14 below experimental values.

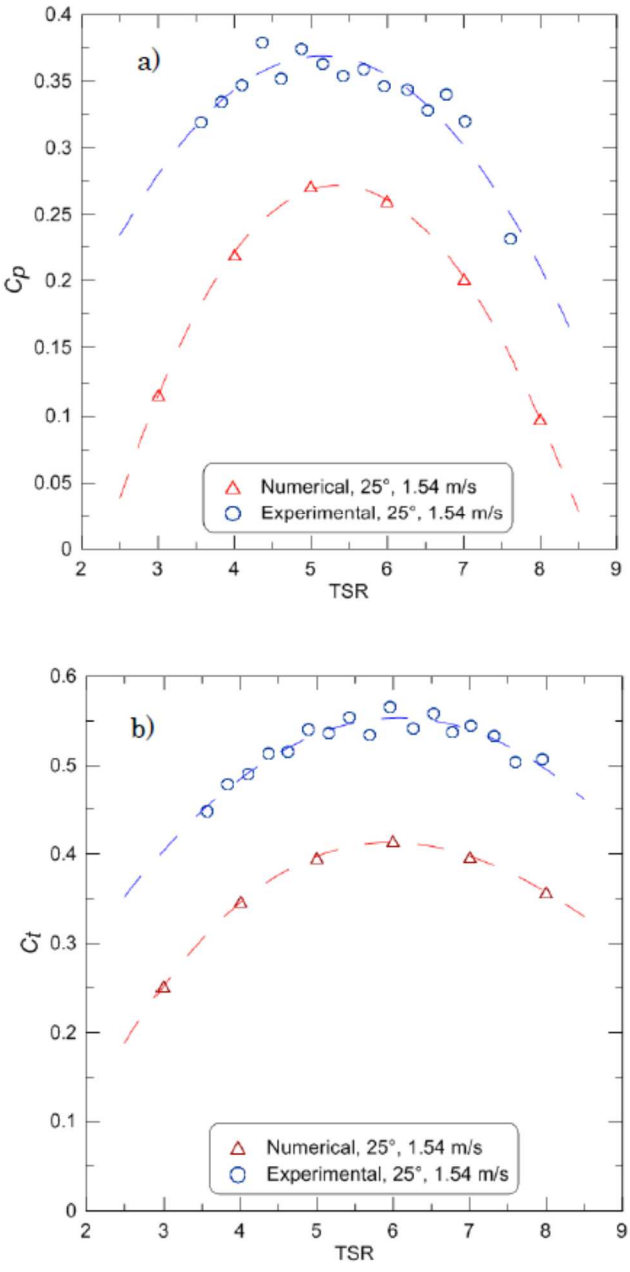

Fig. 7 a) C_p as a function of TSR, b). C_t as a function of TSR.

This under-prediction could be attributed to several factors, of which include the impact of the mesh size, blockage introduced by the smaller numerical domain, lack of a turbine support nacelle structure which might induced an unrealistic stagnation zone behind the turbine hub.

RESULTS AND DISCUSSION

A three dimensional, three bladed, horizontal axis tidal turbine has been successfully modelled using ANSYS-CFX. A preliminary comparison between steady state numerical and experimental results shows a common trend in C_p and C_t with a significant under-prediction of each. This can be attributed to lack of confidence in the computational mesh, an incomplete geometry representation, and that a blockage correction has not been applied to the numerical results.

It is still interesting to look at the computed flow field around and behind the turbine, as well as the calculated torque and power output prediction as presented in Fig. 8. Both results agree with expectations with regards to peak values at TSR of 5 for this setup. The predicted values of torque and power for this setup peak around TSR = 4.5 and 5.5 with values of 13.5 Nm and 250 W, respectively. This is due to the fact that output power is dependent on the turbine rotational velocity. The link between these two is provided in Eq. (4):

$$P = \omega Q \tag{4}$$

where *P, ω, and Q* represent power [W], rotational velocity [rad/s] and output torque [Nm], respectively

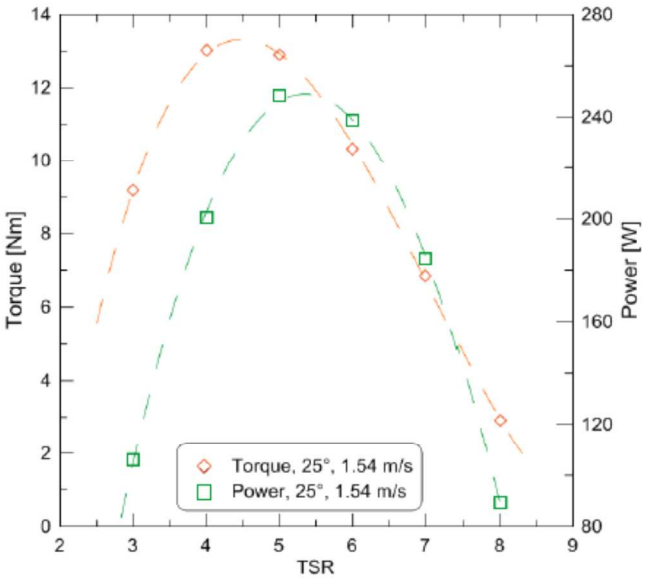

Fig. 8. Torque and power as a function of TSR.

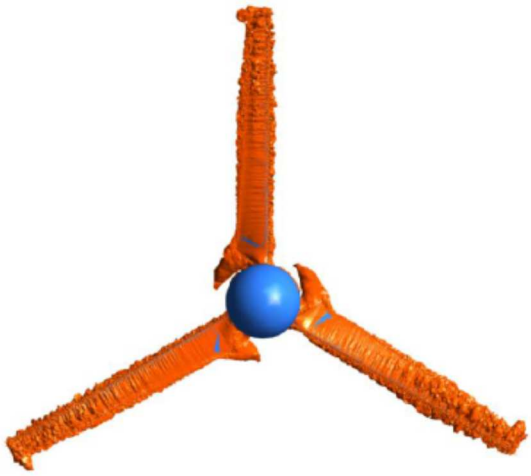

Fig. 9. Absolute helicity on the turbine blade, TSR = 8.

Figure 9 shows the absolute helicity on the turbine at a TSR of 8. There is a focus of vortex creation at both the blade root and tip, two areas of abrupt changes in blade platform. These types of vortices are primary components of wake turbulence and are associated with turbine drag.

The resultant flow field representation on a plane bisecting the middle of the turbine hub for TSR = 5 is provided in Fig. 10. On this vector plot, the colour and length represent flow speed.

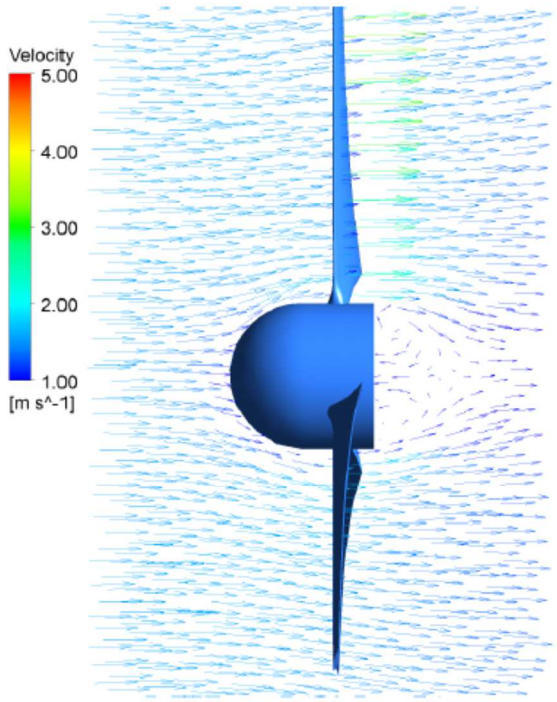

Fig. 10. Vector field around the turbine, TSR = 8.

A stagnation point is observable directly behind the turbine hub. This is unrealistic as the experimental setup included a supported nacelle. Such a stagnation area would induce unrealistic flow patterns that would directly impact the wake propagation downstream. A recirculation area is observed as an effect of this. Future simulations will correct this problem by adding a properly shaped structure behind the turbine hub.

A similar vector field result is provided in Fig. 11 in three dimensions. Divergent flow is observed around the turbine as expected. This flow divergence implies that the turbine is extracting power, creating a local high pressure zone. The high local pressure causes inflow to deflect around the turbine, and reconverge downstream. The distance of this convergence is of interest as it holds implications for tidal turbine arrays.

One method of analyzing the downstream extension of the wake is to observe the vorticity strength at varying distances from the turbine. Figure 12 provides contour plots of resultant vorticity at 0.5*D*, 1*D*, 1.5*D* and 2*D* downstream of the turbine with a TSR = 5. In addition, this figure provides planar velocity vectors as a method of observing downstream fluid movement.

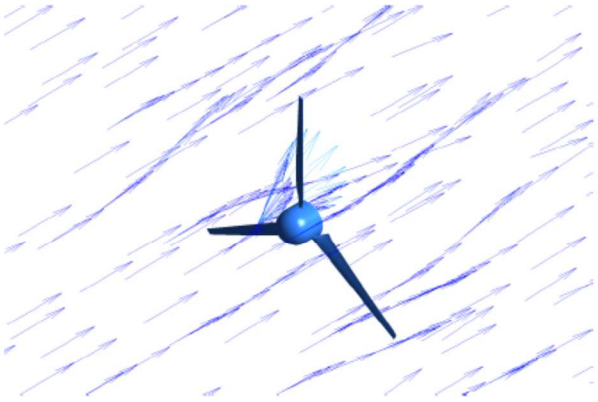

Fig. 11. 3D vector field, TSR = 8.

A local region of high vorticity is seen directly behind the turbine, at a distance of 0.5 *D*. As discussed earlier, the lack of a nacelle creates a stagnation area with a large amount of recirculation. High level of vorticity are observed behind the hub and turbine blade, where the flow in this plane is now rotation counterclockwise, *i.e.*, in the direction opposite the turbine rotation. This is expected for the flow after interaction with the turbine blade.

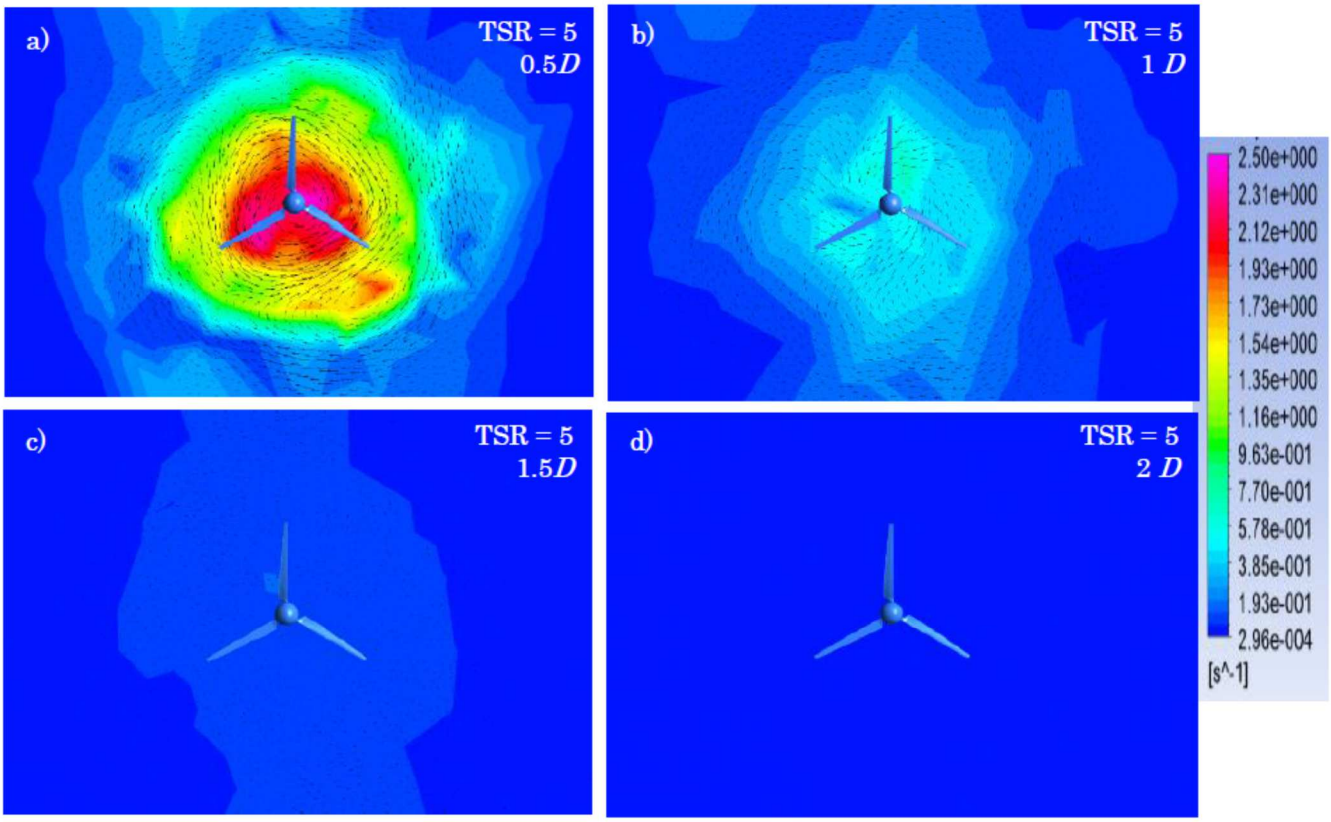

Fig. 12. Vorticity contour plots and planar vector fields at a distance of 0.5, 1, 1.5 and 2 *D* behind the turbine for a TSR = 5 at 1.54 m/s.

Outside of the area delimited in green, the flow direction follows the turbine rotation. There is still a noticeable amount of vorticity extending up to 3 times the diameter of the turbine in this plane. At a distance of 1 *D*, Fig. 12b, the amount of vorticity directly behind the turbine has already decreased vastly, but with impacts still being seen at distances up to 3 *D* away from the center of the turbine. Rotations in the wake is also greatly reduced, although the inner counterclockwise rotation and outer clockwise rotation are still observed. Measurable vorticity diminishes greatly at a distance of 1.5 *D* (Fig. 12c) and completely disappears at a distance of 2 *D* (Fig. 12d).

Figure 13 presents similar vorticity contour plots and vector field in those planes for a TSR = 8. In this case, it is clear that the fastest rotational speed result in an increased amount of vorticity just behind the turbine at 0.5*D* (Fig. 13a). This larger amount of vorticity can be related to the decreased performance of the turbine as shown through C_p (Fig. 7a). Two larger recirculation zone/eddies are also observed past the two lower turbine blade. More importantly, it clearly shows that the impact of the turbine rotation seen through the vorticity extends well beyond the size of the water volume simulated; extended volumes will be used and validated in the continuation of this project. A similar counterclockwise/clockwise flow can also be observed in this situation.

Figure 13b shows the amount of vorticity in a plane situation a distance *D* from the turbine. At this point, the amount of vorticity observed is now mainly found within a distance 2*D* of the turbine center. Figures 13c and d show that this increased vorticity generated by the faster turbine blade velocity persist longer in the flow, although, at 2*D*, most of this vorticity has dissipated and the flow resembles a lot to the one observed for a TSR = 5.

CONCLUSION

A fluid numerical model of a three bladed horizontal axis tidal turbine has been created. The preliminary results of this investigation have been compared with experimental results with reasonable agreement in trends. A significant under-prediction of both C_p and C_t are observed however. A lack of confidence in the computational mesh could be a cause of this as a mesh convergence study has yet to be completed. Other possibly sources of error include the lack of blockage correction in the numerical results as well as an incomplete representation of the physical experimental geometry.

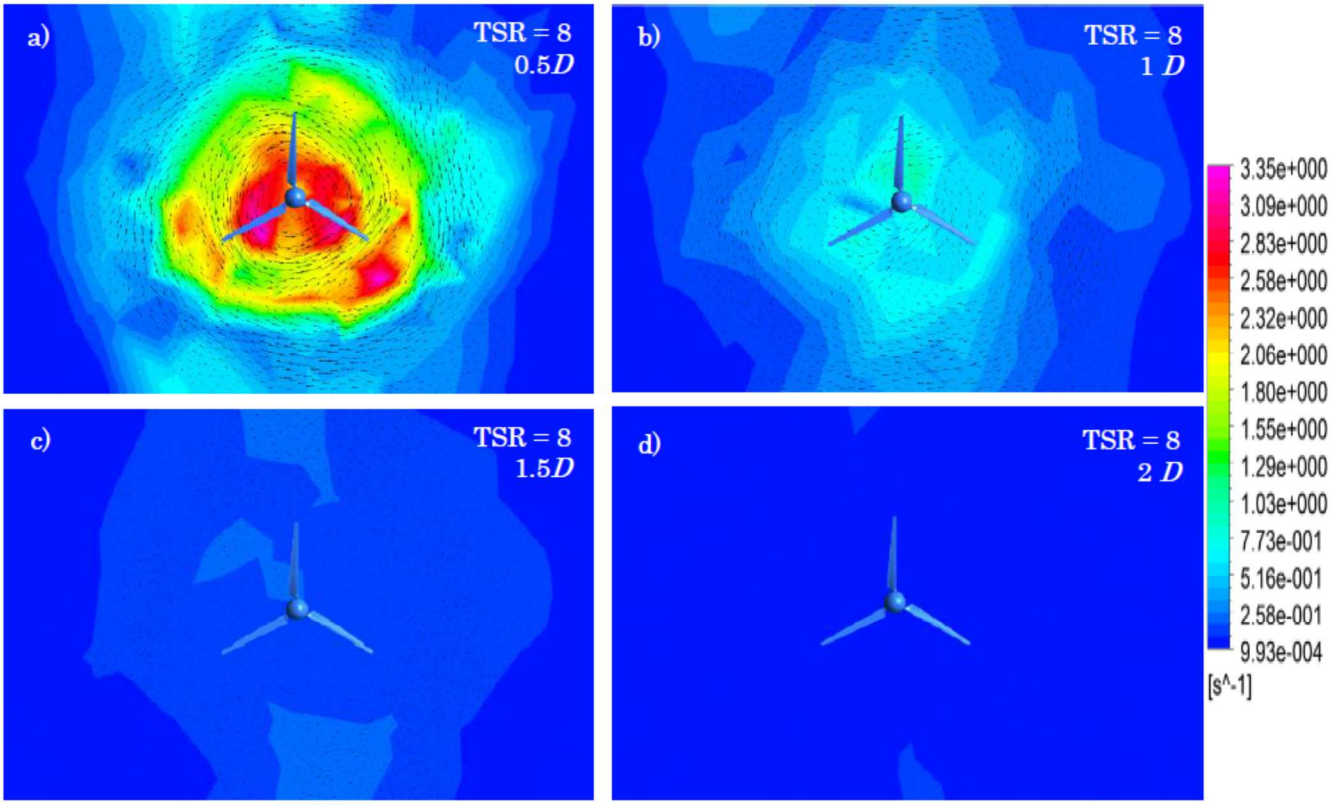

Fig. 13. Vorticity contour plots and planar vector fields at a distance of 0.5, 1, 1.5 and 2 *D* behind the turbine for a TSR = 8 at 1.54 m/s.

A maximum value of C_p was found to be 0.27 at TSR = 5.5, while the experimental peak is 0.37 at TSR = 5. This resulted in an average C_p relative error of 39%. A maximum value of C_t was found to be 0.4 at TSR = 6, while the experimental peak is 0.55 at TSR = 6. More importantly, the trends observed in both C_p and C_t are important as they prove the appropriate flow physics are being accounted for.

Velocity vector plots show the flow deflection around the turbine, as well as recirculation downstream of the hub. This implies that the turbine nacelle should be included in subsequent studies as the current solutions provide unrealistic flow patterns. Also, turbulent effects in the wake propagation seem to diminish after a distance of $2D$ downstream of the turbine in this setup, as shown in Figs. 12 and 13.

The effect of blockage correction is also noted in this study. Subsequent studies will include a larger fluid domain to represent the free-stream correction of Bahaj *et al.* A domain size convergence study will then be completed, in addition to the mesh convergence study.

This preliminary comparison analysis of numerical and experimental investigations show the applicability of this computational method for a tidal turbine scenario. Additional work, which has been discussed previously, will be completed, the results of which will be further disseminated.

ACKNOWLEDGEMENTS

The authors are grateful to the Offshore Energy Research Association (OERA) of Nova Scotia, the Natural Science and Engineering Research Council (NSERC) of Canada and the Canadian Foundation for Innovation (CFI) for their financial support for this work.

Additionally, the authors would like to thank Philip Marsh at the University of Tasmania's Australian Maritime College, and Aidan Bharath at Dalhousie University for their advice.

REFERENCES

[1] R. H. Karsten et al., "Assessment of tidal current energy in the Minas Passage, Bay of Fundy", *Proceedings of the Institution of Mechanical Engineers, Part A: Journal of Power and Energy*. **222**. 2008, pp. 493-507.

[2] Md. J. Alam and M. T. Iqbal, "A low cut-in speed marine current turbine", *Journal of Ocean Technology*. **5**, 2010, pp. 14-49.

[3] B. K. Kirke, "Tests on ducted and bare helical and straight blade Darrieus hydrokinetic turbines", *Renewable Energy*. **36**, 2011, pp. 3013-3022.

[4] W. M. J. Batten et al., "The prediction of the hydrodynamic performance of marine current turbines", *Renewable Energy*. **33**, 2008, pp. 1085-1096.

[5] R. McSherry et al., "3D CFD modelling of tidal turbine performance with validation against laboratory experiments", *Proceedings of the 9th European Wave and Tidal Energy Conference*. 2011.

[6] T. O'Doherty et al., "Experimental and Computational Analysis of a Model Horizontal Axis Tidal Turbine", *Proceedings of the 8th European Wave and Tidal Energy Conference*. 2009, pp. 833-841.

[7] M. E. Harrison et al., "A comparison between CFD simulations and experiments for predicting the far wake of horizontal axis tidal turbines", *Proceedings of the 8th European Wave and Tidal Energy Conference*. 2009, 566-575.

[8] A. S. Bahaj et al., "Power and thrust measurements of marine current turbines under various hydrodynamic flow conditions in a cavitation tunnel and a towing tank", *Renewable Energy*. **32**, 2007, pp. 407-426.

Appendix C

EWTEC 2015 – Abstract

3D modeling of a Tidal Turbine – An Investigation of Wake Phenomena

Nick Osbourne[#1], Dominic Groulx[#2], Irene Penesis[*3]

[#]*Department of Mechanical Engineering, Dalhousie University*
Halifax, Nova Scotia, Canada
[1]nick.a.osbourne@dal.ca
[2]dominic.groulx@dal.ca

[*]*Australian Maritime College, University of Tasmania*
Launceston, Tasmania, Australia
[3]i.penesis@utas.edu.au

I. KEYWORDS

Computational Fluid Dynamics (CFD), Horizontal Axis Tidal Turbines (HATT), Shear Stress Transport (SST), Reynolds Averaged Navier-Stokes (RANS), Tip Speed Ratio (TSR).

II. ABSTRACT

With the rise of renewable energy industries, their success depends on their environmental and economic sustainability. For tidal energy, many believe that large scale farms must be developed for it to become a financially viable industry. As in the case for wind farms, turbine interaction through wake shadowing effects can severely impact their performance, and thus the farm as a whole. There is minimal knowledge to date on the wake recovery from a tidal turbine. This abstract presents the continuation of work presented at AWTEC 2014 [1] which aspired to investigate this area by numerically modelling a turbine for comparison with experimental results.

Actuator disc method is a popular tool in wake modelling but lacks in near field detail in the wake region. The knowledge of these physics will speak to main contributors of wake vorticity as well as key areas of structural loading. For this reason, a fully resolved 3D geometry was chosen for analysis. The HATT geometry that was chosen has a design that matches experimental studies from the University of Southampton [2] for validation purposes. The 800 mm diameter turbine has a blade geometry that is based on five NACA profiles and can be seen in Fig. 1.

Fig. 1 Turbine and Nacelle Geometry

CFD simulations were ran in ANSYS CFX using an unstructured tetrahedral mesh. Refinement around the turbine is such that $y+ \approx 1$. A RANS solver approach was taken, incorporating the SST turbulence model. Flow cases consisted of a range of TSR (2-12) and V_0 (0.8-2 m/s). Both power and thrust coefficients, C_P and C_T, were monitored and used for comparison to experimental values. Overall, the result trends matched but both parameters were under-estimated. More details can be found in [1].

There are many post-processing techniques that can be used to examine flow within the wake. Contour plots are a commonly used visualization tool which can represent results such as: velocity and pressure gradients, turbulent intensity and wake recovery distances. 3D helicity gives insight into vortex creation at, and directly behind, the turbine. Velocity deficit is valuable wake analysis tool which is a non-dimensional number relating downstream (V_w) and free stream (V_0) velocities. Figure 2 is an example of this deficit, which is defined as:

$$V_{deficit} = 1 - \frac{V_w}{V_0} \quad (1)$$

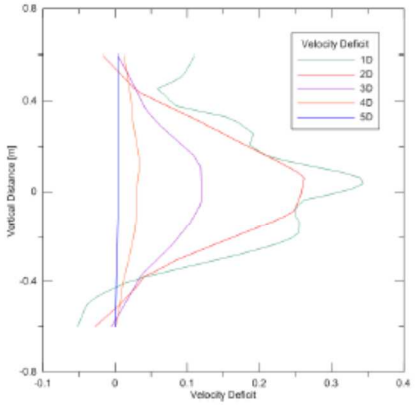

Fig. 2 Velocity Deficit – TSR = 5, V_0 = 1.54 m/s

This approach, along with contour plot analysis gives insight into wake recovery distances and turbulent intensity. Further work is underway to improve result comparison.

REFERENCES

[1] Osbourne, N., D. Groulx, and I. Penesis. *Three Dimensional Simulation of a Horizontal Axis Tidal Turbine - Comparison with Experimental Results*. in *2nd Asian Wave and Tidal Energy Conference (AWTEC)*. 2014. Tokyo, Japan.

[2] Bahaj, A.S., et al., *Power and thrust measurements of marine current turbines under various hydrodynamic flow conditions in a cavitation tunnel and a towing tank*. Renewable Energy, 2007. **32**(3): p. 407-426.